Published in final edited form as:
Mol Cancer Ther. 2014 February ; 13(2): 426–432. doi:10.1158/1535-7163.MCT-13-0633.

The effect of photoimmunotherapy (PIT) followed by liposomal daunorubicin in a mixed tumor model: A demonstration of the super enhanced permeability and retention (SUPR) effect after PIT

Kohei Sano, **Takahito Nakajima**, **Peter L. Choyke**, and **Hisataka Kobayashi***
Molecular Imaging Program, Center for Cancer Research, National Cancer Institute, National Institutes of Health, Bethesda Maryland 20892, United States

Abstract

In general, *de novo* solid tumors are composed of phenotypically and functionally heterogeneous malignant cells. This heterogeneity interferes with the effectiveness of targeted molecular cancer therapies. Even if most of the tumor is killed by a targeted treatment, recurrences are common and can be lethal. In this study, a mixed tumor model, which is predominantly a population of epidermal growth factor receptor (EGFR)-positive A431 cells combined with a smaller population of EGFR-negative Balb3T3/deRed cells, was established. This mixed tumor was then treated with photoimmunotherapy (PIT), a newly developed target-cell selective cancer therapy using a monoclonal antibody (mAb)-photosensitizer (IR700 fluorescence dye) conjugate and exposure of near infrared light. While PIT successfully treated EGFR-positive A431 cells in the mixed tumor, EGFR negative Balb/DsRed cells were not responsive. However, PIT also induced a large increase in tumor permeability known as the SUPR effect, which allowed a 5-fold increase in the accumulation of a liposomal chemotherapy (DaunoXome) and resulted in more effective therapy than either PIT or liposomal daunorubicin alone. The liposomal daunorubicin, administered 1 h after EGFR-targeted PIT, was homogeneously distributed allowing delivery to tiny surviving nests of EGFR-negative Balb3T3/DsRed cells resulting in prolonged survival of mice.

Keywords

tumor heterogeneity; targeted cancer therapy; photoimmunotherapy; nano-delivery; super-enhanced permeability and retention effects

INTRODUCTION

Solid tumors are composed of phenotypically and functionally heterogeneous malignant cells (1, 2), which arise from genetic (3) or epigenetic changes (4), or are a response to local environmental stresses such as hypoxia (5). Heterogeneity interferes with the effectiveness of cancer therapies, especially when targeted molecular therapies are employed. Even if most of the tumor is killed by a targeted treatment, recurrences are common and can be lethal.

*For correspondence or reprints contact: Hisataka Kobayashi, M.D., Ph.D. Molecular Imaging Program, Center for Cancer Research, National Cancer Institute, NIH, Building 10, RoomB3B69, MSC1088, Bethesda, MD 20892-1088. Phone: 301-435-4086, Fax: 301-402-3191. Kobayash@mail.nih.gov.

There is no conflict of interest to be disclosed for all authors listed.

Studying tumor heterogeneity in animal models is difficult. A fundamental limitation of most implanted cell lines is that are much less heterogeneous than *de novo* lesions and therefore, do not reflect this common and important characteristic of spontaneous cancers. Transgenic mouse cancer models, can simulate cancers in patients better than any other models, attempt to overcome this problem, however, the variable timing for establishing a tumor make transgenic models inefficient and expensive to work with. Another approach is to use actual intact tumor explants, however, it is difficult to get uniform results across a population of animals since every explants is unique. Thus, there is a need for simpler tumor models that take into account tumor heterogeneity but are reproducible, efficient and less costly than transgenic or explant models.

In this work, a mixed tumor model, which is predominantly a population of epidermal growth factor receptor (EGFR)-positive cells combined with a smaller population of EGFR-negative cells, was established. This mixed tumor was then treated with photoimmunotherapy (PIT), a newly developed cancer therapy using a monoclonal antibody (mAb)-photosensitizer (IR700 fluorescence dye) conjugate (6). Immediate and massive necrotic cell death is commonly seen only in target-expressing cancer cells after exposure to near-infrared (NIR) light. Following PIT the tumor demonstrates dramatically increased permeability (a phenomenon termed super enhanced permeability and retention or SUPR) for nano-sized anti-cancer drugs including liposomal daunorubicin, which further enhances killing of cancer cells. Because PIT is so specific for the targeted cell, with virtually no bystander effect, it is ideal to study in a multi-cell line tumor model. In this study we investigate the effect of PIT in a tumor model in which two cell lines are mixed and implanted. We then investigate the effect of liposomal daunorubicin on the cells remaining after effective PIT has been delivered.

MATERIALS AND METHODS

Reagents

A water-soluble, silicon-phthalocyanine derivative, IRDye 700DX NHS ester (IR700) was purchased from LI-COR Bioscience (Lincoln, NE). Panitumumab (Pan), a fully humanized IgG2 mAb directed against extracellular domain of the human epidermal growth factor receptor (EGFR) 1 (HER1), was purchased from Amgen (Thousand Oaks, CA). Liposomal daunorubicin (DaunoXome; DX) was purchased from Galen US Inc. (Souderton, PA). All other chemicals used were of reagent grade.

Cells

EGFR-expressing A431 cells and Balb3T3/DsRed (Balb/DsRed) cells (7, 8) were used for PIT. A431, which is a human epidermoid carcinoma cell line (9), and Balb3T3, which is a virally transformed mouse 3T3 embryonic fibroblast cell line by virus infection, were purchased from ATCC (Manassas, VA). Balb3T3 was transfected DsRed-express plasmid (Clonetech, Mountain View, CA) in house. Cells were grown in RPMI1640 supplemented with 10% fetal bovine serum and 1% penicillin/streptomycin in tissue culture flasks in a humidified incubator at 37°C in an atmosphere of 95% air and 5% carbon dioxide. Both cells have been passaged in our lab within 4 months.

Synthesis of panitumumab-IR700 conjugates

Conjugation of Pan with IR700 was performed according to the procedure reported previously. In brief, Pan (1 mg, 6.8 nmol) was incubated with IR700 (66.8 μg, 34.2 nmol) in 0.1 M aqueous Na2HPO4 (pH 8.6) at room temperature for 1 h. The mixture was purified with a Sephadex G50 column (PD-10; GE Healthcare). The number of IR700 per mAb was approximately four.

Animal models

All *in vivo* procedures were carried out in compliance with the Guide for the Care and Use of Laboratory Animal Resources (1996), U.S. National Research Council, and approved by the National Cancer Institute/NIH Animal Care and Use Committee. Six-eight-week-old female homozygote athymic nude mice were purchased from Charles River (National Cancer Institute Frederick). The mixture of A431 (1×10^6) and Balb/DsRed cells (1×10^4) was injected subcutaneously in the right and left dorsi under isoflurane anesthesia, and the experiments were conducted 3–5 days after cell injection. In order to investigate the population of EGFR+ tumor cells before and after PIT, mice were initially injected with Pan-IR700 (100 μg) intravenously, and 1 d later, the tumor was irradiated with NIR light from a red-light-emitting diode at wavelengths of 670–710 nm and a power density of 50 J/cm^2, as measured with an optical power meter (PM 100 (Thorlabs)), and the PIT-treated tumors were excised and frozen 0, 1, and 7 d after PIT. Pan-IR700 was re-injected on day 6 after PIT and the animal was re-exposed to NIR light at the same dose, before tissue harvesting on day 7. Ten-μm-thick frozen sections were prepared and fluorescence was assessed using an Olympus BX61 microscope (Olympus America, Inc., Melville, NY) equipped with the following filters: excitation wavelength 590 to 650 nm and 480 to 550 nm, emission wavelength 662.5 to 747.5 nm, and 590 nm long pass for IR700 and DsRed, respectively. Transmitted light differential interference contrast images were also acquired. Furthermore, to evaluate histological changes after PIT with NIR light, the tumors (A431+Balb/DsRed) treated with PIT by exposing 0 and 50 J/cm^2 of NIR light were harvested in 10% formalin 1 h after PIT. Serial three 10-mm slice sections were fixed on a glass slide with H&E staining.

In vivo fluorescence imaging studies after PIT

Five days after cell injection, 100 μg of Pan-IR700 was administered intravenously, and 1 d later, one tumor was irradiated with NIR light (50 J/cm^2) while the other side was shielded from light using aluminum foil. One hour after PIT, liposomal daunorubicin (DX) (30 mg/kg) was injected intravenously, and *in vivo* fluorescence images were obtained with a Maestro Imager (CRi) using a band-pass filter from 503 to 555 nm (excitation) and a long-pass green filter over 580 nm (emission). The tunable emission filter was automatically stepped in 10 nm increments from 500 to 800 nm for the green filter sets at constant exposure. The spectral fluorescence images consist of autofluorescence spectra and the spectra from daunorubicin, which were then unmixed, based on the characteristic spectral pattern of daunorubicin, using commercial software (Maestro software; CRi). Regions of interest (ROIs) were manually drawn on both tumors and the normal back of the mouse, and the fluoresence intensity was calculated. The tumors were excised and frozen for fluorescence microscopy. The fluorescence was assessed using an Olympus BX61 microscope equipped with the following filters: excitation wavelength 590 to 650 nm, 480–550 nm, and 480–550 nm, emission wavelength 662.5 to 747.5 nm, 590 nm long pass, and 590 nm long pass for IR700, DsRed, and daunorubicin, respectively. Spectral data of different reagents was separated using Maestro software (CRi). Transmitted light differential interference contrast images were also acquired.

In vivo therapeutic studies based on the SUPR effect

The mixed tumor cells (A431 and Balb/DsRed) were injected s.c. in the right flank of the mice. In order to determine the tumor volume, the greatest longitudinal diameter (length) and the greatest transverse diameter (width) were determined with an external caliper. Tumor volume based on caliper measurements was calculated using the following formula: $\text{tumor volume} = \text{length} \times \text{width}^2 \times 0.5$ (8). Tumors reaching approximately 40 mm^3 in volume were selected for the study. Selected mice were randomized into 4 groups of at least

10 mice per group for the following treatments: (1) no treatment; (2) liposomal daunorubicin (6 mg/kg); (3) PIT (50 J/cm^2); (4) PIT (50 J/cm^2), followed by liposomal daunorubicin (6 mg/kg) 1 h later. After treatment, the mice were monitored daily, and their tumor volume was measured twice a week until it reached 1300 mm^3, at which time mice were euthanized with carbon dioxide gas.

Statistical analysis

Data are expressed as means ± s.e.m. from a minimum of three experiments, unless otherwise indicated. Statistical analyses were carried out using a statistics program (Statview). For multiple comparisons, a one-way analysis of variance (ANOVA) followed by Tukey-Kramer test was used. The cumulative probability of survival, determined herein as the tumor volume failing to reach 1300 mm^3, was estimated in each group with the use of the Kaplan Meier survival curve analysis, and the results were compared with the log-rank test with Bonferroni's correction for multiple comparisons. $p < 0.05$ was considered to indicate a statistically significant difference.

RESULTS

Establishment of mixed tumor model

Inoculation of the mixture of A431 and Balb/DsRed cells produced tumors in which the majority of the cells were derived from EGFR+ A431 cells while small islands of Balb/DsRed cells became visible 3–5 days after innoculation (Figure 1). Pan-IR700 specifically accumulated in regions of DsRed-negative A431 tumor cells. NIR light exposure induced immediate and massive necrosis of A431 cells but did not affect EGFR-negative Balb/DsRed cells (Figure 1). As a consequence the proportion of Balb/DsRed cells in the tumors gradually increased as a function of time after EGFR-targeted PIT, and by 7days the tumor was completely dominated by Balb/DsRed cells (Figure 1).

In vivo dynamic fluorescence imaging after PIT

In order to evaluate the increased delivery of liposomal daunorubicin into tumors following PIT, commercially available liposomal daunorubicin (DaunoXome; DX, mean diameter 50 nm) was administered 1 h after treatment with EGFR-targeted PIT. Based on the inherent fluorescence of daunorubicin, optical imaging showed that DX rapidly accumulated and diffused into PIT-treated tumors within 30 min after injection but not into untreated tumors (Figure 2A, B). The ratios of fluorescence signal intensity at 30 min was 5-fold higher in the PIT-treated tumor compared with the control tumor using the following equation: $(\mathrm{SI}_{\mathrm{PIT\ at\ 30\ min}} - \mathrm{SI}_{\mathrm{Background\ at\ 30\ min}})/(\mathrm{SI}_{\mathrm{Control\ at\ 30\ min}} - \mathrm{SI}_{\mathrm{Background\ at\ 30\ min}})$. (Figure 2C). IR700 fluorescence in PIT-treated tumor decreased due to washing out the antibody-IR700 conjugate from killed tumor cells and photo-bleaching (Figure 2A). DX was widely distributed throughout the tumor including those areas occupied by Balb/DsRed cells (Figure 2D).

Therapeutic studies

A431 tumors were treated with a single dose of light (50 J/cm^2) 1 d after injection of Pan-IR700. We compared the efficacy of treatment in four groups of mice bearing mixed A431 and Balb/DsRed tumors ($n \geq 10$ in each group). All treated tumors had a volume of less than 1300 mm^3, in accordance with our institution's animal care and use guidelines. All but 5 mice were euthanized when their tumors exceeded 1300 mm^3,. Tumor volume was significantly reduced when treated with the combination of PIT and DX, compared with untreated control mice or mice treated with DX or PIT alone (Figure 3A), and survival was

significantly prolonged in mice with the combination therapy of PIT and DX compared to all other groups (Figure 3B).

DISCUSSION

PIT, using panitumumab-IR700, showed a robust therapeutic effect on EGFR-expressing A431 tumor cells, while EGFR-negative tumor cells (Balb/DsRed) remained viable and eventually became the dominant cell type. PIT quickly killed EGFR-expressing cells within minutes after NIR light exposure. PIT induced irreversible cellular membrane damage that allowed extracellular water to enter into cells resulting in swelling, blebbing and bursting of the cells(6). Although the mechanism of PIT remains unclear, none of the singlet oxygen quenchers or reducing agents including sodium azide, Glutathione, 4-hydroxy-2,2,6,6-tetramethylpiperidin-1-oxyl (TEMPOL), etc. interfered with the efficacy of PIT, suggesting a mechanism other than singlet oxygen (Type 2 reaction). However, the actual mechanism of cell membrane injury remains unclear. Because PIT leaves the vasculature intact and the perivascular tumor cells are rapidly killed by PIT, there is a sudden increase in vascular permeability, especially for larger molecules (10). Nano-sized reagents, in this case, liposomal daunorubicin was administered after PIT and homogeneously distributed within the tumor at 5-fold concentrations in the normal tumor based on contralateral non-treated controls. The combination of PIT and liposomal daunorubicin increased the survival of mice compared with either PIT or liposomal daunorubicin alone.

In previous work, EGFR-targeted PIT using panitumumab-IR700 with repeated NIR exposures was able to cure >80% of A431 tumors with PIT alone (11). However, an unrealistic feature of this model is that the monoclonal A431 cells homogeneously expressed high levels of EGFR whereas most tumors contain mixtures of antigen positive and antigen negative cells. Therefore, the mixed tumor model described here which contains both EGFR-positive A431 and EGFR-negative Balb/DsRed cells provides more insight into how actual tumors might respond to PIT and how they might be treated with adjuvant liposomal chemotherapies. In this work, we demonstrate that, in contrast to a clonal xenograft model, the mixed tumor model responds better to a combination of therapies rather than PIT or liposomal cancer therapy alone.

PIT can kill the majority of target-positive cells, however target-negative cells will be unaffected. Eventually, regrowth will occur with antigen negative cells. However, PIT induces a super enhanced permeability and retention (SUPR) effect that preferentially allows the accumulation of nano-sized reagents in the tumor bed. In PIT the layers of tumor cells adjacent to tumor vessels are killed first while the endothelial cells are undamaged leading to intact but dilated vessels which are highly permeable (10). This effectively targets non-specific nano-sized reagents to the remaining target negative tumor cells. We demonstrate a 5-fold increase in liposomal daunarubicin concentration within PIT treated tumors compared with untreated tumors. This benefit should accrue to any nano-sized reagent and is not specific for liposomal daunorubicin. Thus PIT enables the use of a broad spectrum of nano-sized therapies hitherto limited by enhanced permeability and retention (EPR) effects that are on the order of 1.1–1.5 fold higher than background. Scattered cancer cells generally are more susceptible to cancer treatments as the most common barriers to drug delivery are reduced. Thus, the SUPR effect following PIT offers opportunities for the utilization of more nano-sized reagents than are currently in use. Therefore, combining PIT and nano-sized reagents is theoretically a highly complementary approach for heterogeneous tumors including treatment of cancer stem-like cells.

A potential alternative would be to use fluorescent proteins (FPs), which are excellent endogenous fluorescence emitters and/or singlet oxygen producers. Potentially these could

be used for depicting various biological processes or for killing FP-expressing cells, respectively, both in vitro and in vivo. Another recently reported technology is the use of telomerase promoter-regulated expression of various fluorescent proteins, which are induced with adenovirus-mediated gene transfection *in vivo* (12–15). However, the requirement for virus-mediated *in vivo* gene transfection, makes it unlikely to be translated for human use in the near term. In contrast, the PIT technology described here should be readily translatable as it requires the injection of an antibody-IR700 conjugate and exposure to non-thermal levels of NIR light.

It has been reported that conventional photodynamic therapy (PDT) can also enhance the delivery of various nano-sized or macromolecular drugs up to 3-fold compared with control tumor between 0 and 12 hours after PDT depending on the dose (16–18). Photosensitizers including verteporfin show preferential retention in the tumor vasculature and tumor cells. Histological analysis did not clearly explain the enhanced drug delivery. However, the preponderance of reports suggest that PDT destroys morphological changes on endothelial cells (18) or the structure of tumor vasculature (16) leading to a transient enhancement of tumor vasculature permeability after low doses of photosensitizer and light exposures with appropriate intervals. The enhanced permeability induced by conventional PDT seems to be a dynamic process, therefore, the effective dose of PDT usually damages both tumor and vascular cells resulting in reductions in blood flow (19, 20), which enhances its anti-tumor effects. In contrast, in PIT, antibody-IR700 conjugates selectively bind to target-positive tumor cells with minimal non-target cell uptake of IR700 inducing rapid necrotic damage especially on cancer cells near vessels thus, causing dilatation of tumor vessels and dramatically increasing permeability. We have termed this the SUper-enhanced Permeability and Retention or SUPR effect, which has been shown to increase the delivery of nano-particles up to 24-fold compared with control tumors where only conventional enhanced permeability and retention (EPR) is observed (10). Anti-EGFR antibodies alone did not induce SUPR effects in EGFR-positive tumors. The SUPR effect induced by PIT is not specific for EGFR expressing tumors but can be seen with a variety of mAb-IR700 conjugates including anti-HER2-IR700. However, receptor negative cells are unaffected because the hydrophilicity of IR700 prevents binding to cells without the appropriate mAb. When comparing the enhanced permeability with PDT to PIT, micro-drug distribution after PDT showed that the nano-drugs were located only near blood vessels (16, 18), while after PIT, daunorubicin was homogeneously delivered into both the expressing and non-expressing parts of the tumor. Therefore, of the magnitude of SUPR effects induced by PIT is greater than the enhanced drug delivery after PDT.

CONCLUSION

A mixed tumor model containing EGFR-positive and negative tumor cells was established to better understand the effects of PIT in heterogenous cancer cell populations. While PIT successfully treated EGFR-positive A431 cells, EGFR negative Balb/DsRed cells were not responsive and eventually became the dominant cell. However, PIT also induced a large increase in tumor permeability, (also known as the SUPR effect), which allowed a 5-fold increase in the accumulation of an adjuvant liposomal chemotherapy (DaunoXome) and resulted in more effective therapy than either PIT or liposomal daunorubicin alone. The liposomal daunorubicin administered 1 h after EGFR-targeted PIT was homogeneously distributed allowing delivery to and killing of EGFR-negative Balb/DsRed cells resulting in prolonged survival of mice.

Acknowledgments

This research was supported by the Intramural Research Program of the NIH, National Cancer Institute, Center for Cancer Research.

References

1. Fidler IJ, Kripke ML. Metastasis results from preexisting variant cells within a malignant tumor. Science. 1977; 197:893–5. [PubMed: 887927]
2. Fidler IJ, Hart IR. Biological diversity in metastatic neoplasms: origins and implications. Science. 1982; 217:998–1003. [PubMed: 7112116]
3. Nowell PC. Mechanisms of tumor progression. Cancer Res. 1986; 46:2203–7. [PubMed: 3516380]
4. Baylin SB, Jones PA. A decade of exploring the cancer epigenome - biological and translational implications. Nat Rev Cancer. 2011; 11:726–34. [PubMed: 21941284]
5. Bissell MJ, Hines WC. Why don't we get more cancer? A proposed role of the microenvironment in restraining cancer progression. Nat Med. 2011; 17:320–9. [PubMed: 21383745]
6. Mitsunaga M, Ogawa M, Kosaka N, Rosenblum LT, Choyke PL, Kobayashi H. Cancer cell-selective in vivo near infrared photoimmunotherapy targeting specific membrane molecules. Nat Med. 2011; 17:1685–91. [PubMed: 22057348]
7. Koyama Y, Hama Y, Urano Y, Nguyen DM, Choyke PL, Kobayashi H. Spectral fluorescence molecular imaging of lung metastases targeting HER2/neu. Clin Cancer Res. 2007; 13:2936–45. [PubMed: 17504994]
8. Barrett T, Koyama Y, Hama Y, Ravizzini G, Shin IS, Jang BS, et al. In vivo diagnosis of epidermal growth factor receptor expression using molecular imaging with a cocktail of optically labeled monoclonal antibodies. Clin Cancer Res. 2007; 13:6639–48. [PubMed: 17982120]
9. Giard DJ, Aaronson SA, Todaro GJ, Arnstein P, Kersey JH, Dosik H, et al. In vitro cultivation of human tumors: establishment of cell lines derived from a series of solid tumors. J Natl Cancer Inst. 1973; 51:1417–23. [PubMed: 4357758]
10. Sano K, Nakajima T, Choyke PL, Kobayashi H. Markedly enhanced permeability and retention effects induced by photo-immunotherapy of tumors. ACS Nano. 2013; 7:717–24. [PubMed: 23214407]
11. Mitsunaga M, Nakajima T, Sano K, Choyke PL, Kobayashi H. Near-infrared theranostic photoimmunotherapy (PIT): repeated exposure of light enhances the effect of immunoconjugate. Bioconjug Chem. 2012; 23:604–9. [PubMed: 22369484]
12. Kimura H, Lee C, Hayashi K, Yamauchi K, Yamamoto N, Tsuchiya H, et al. UV light killing efficacy of fluorescent protein-expressing cancer cells in vitro and in vivo. J Cell Biochem. 2010; 110:1439–46. [PubMed: 20506255]
13. Tsai MH, Aki R, Amoh Y, Hoffman RM, Katsuoka K, Kimura H, et al. GFP-fluorescence-guided UVC irradiation inhibits melanoma growth and angiogenesis in nude mice. Anticancer Res. 2010; 30:3291–4. [PubMed: 20944099]
14. Momiyama M, Suetsugu A, Kimura H, Kishimoto H, Aki R, Yamada A, et al. Fluorescent proteins enhance UVC PDT of cancer cells. Anticancer Res. 2012; 32:4327–30. [PubMed: 23060554]
15. Momiyama M, Suetsugu A, Kimura H, Kishimoto H, Aki R, Yamada A, et al. Imaging the efficacy of UVC irradiation on superficial brain tumors and metastasis in live mice at the subcellular level. J Cell Biochem. 2013; 114:428–34. [PubMed: 22961687]
16. Gil M, Bieniasz M, Seshadri M, Fisher D, Ciesielski MJ, Chen Y, et al. Photodynamic therapy augments the efficacy of oncolytic vaccinia virus against primary and metastatic tumours in mice. Br J Cancer. 2011; 105:1512–21. [PubMed: 21989183]
17. Snyder JW, Greco WR, Bellnier DA, Vaughan L, Henderson BW. Photodynamic therapy: a means to enhanced drug delivery to tumors. Cancer Res. 2003; 63:8126–31. [PubMed: 14678965]
18. Chen B, Pogue BW, Luna JM, Hardman RL, Hoopes PJ, Hasan T. Tumor vascular permeabilization by vascular-targeting photosensitization: effects, mechanism, and therapeutic implications. Clin Cancer Res. 2006; 12:917–23. [PubMed: 16467106]

19. Standish BA, Lee KK, Jin X, Mariampillai A, Munce NR, Wood MF, et al. Interstitial Doppler optical coherence tomography as a local tumor necrosis predictor in photodynamic therapy of prostatic carcinoma: an in vivo study. Cancer Res. 2008; 68:9987–95. [PubMed: 19047181]

20. Standish BA, Jin X, Smolen J, Mariampillai A, Munce NR, Wilson BC, et al. Interstitial Doppler optical coherence tomography monitors microvascular changes during photodynamic therapy in a Dunning prostate model under varying treatment conditions. J Biomed Opt. 2007; 12:034022. [PubMed: 17614730]

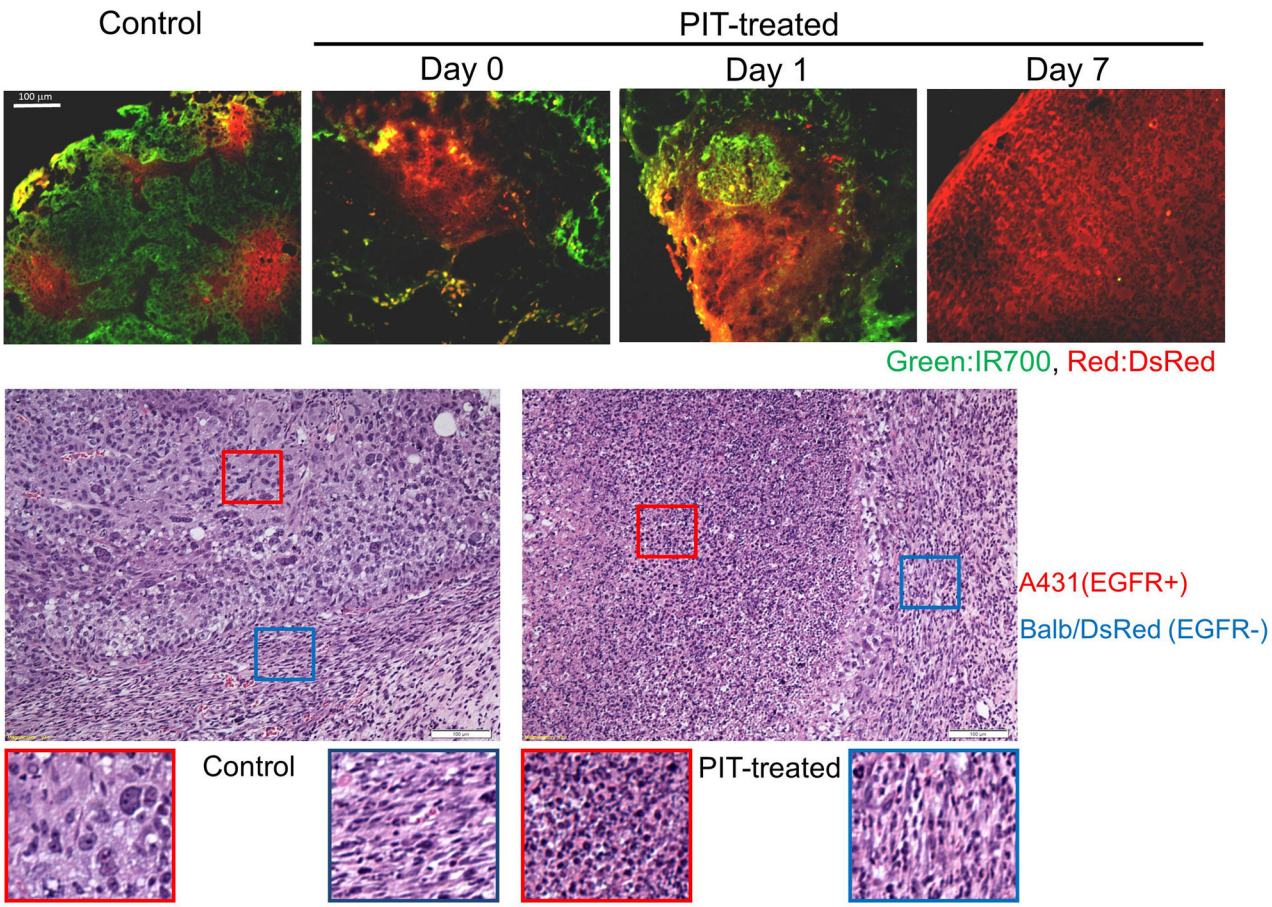

Figure 1.

The mixed tumor model composed of EGFR-positive (A431) and EGFR-negative (Balb/DsRed) tumor cells. Pan-IR700 (green) was intravenously injected 1 d before PIT. Scattered Balb/DsRed tumor foci (red) were observed in A431 cells (Green) before PIT. After PIT, severe damage was shown only in EGFR-positive A431 tumors, and the proportion of Balb/DsRed increased with time after PIT. Balb/DsRed cells eventually almost replaced the entire tumor at 7 days after PIT. Histological evaluation before and after PIT. EGFR-targeted PIT induced selective intense necrosis of EGFR-positve A431 cells as indicated by hematoxylin and eosin (H&E) staining. In contrast, spindle shaped Balb/DsRed cells remain intact even after PIT.

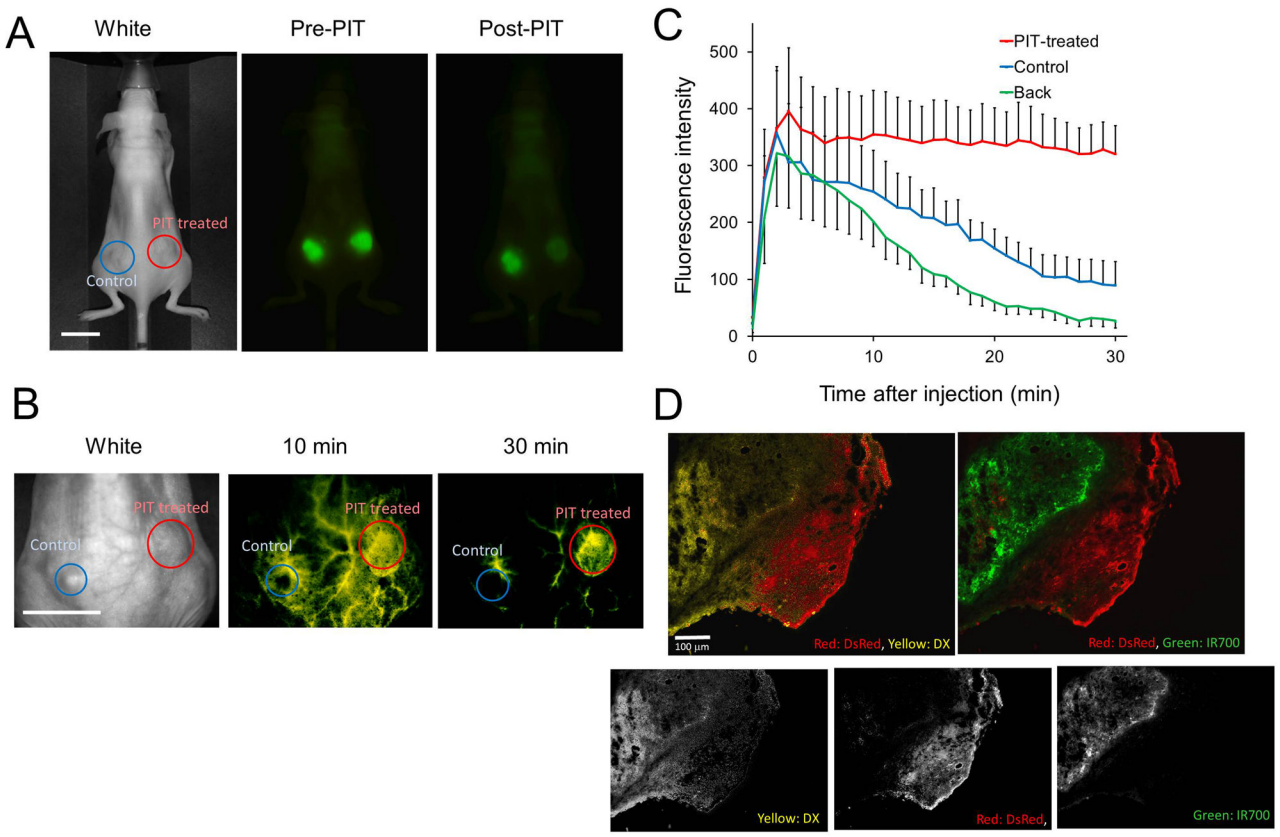

Figure 2.

Enhanced delivery of liposomal daunorubicin based on PIT-induced SUPR effects. (A) *In vivo* fluorescence images of Pan-IR700 (green). PIT was performed only on the right-side tumor with the left-side tumor serving as a control. (B) Liposomal daunorubicin (yellow) preferentially accumulated in PIT-treated mixed tumors (red circles) at 30 min post injection of liposomal daunorubicin, but did not accumulate in no NIR light exposure control tumors (blue circles) growing in the same mice. (C) Dynamic fluorescence intensity curves show that daunorubicin accumulated and was retained by PIT-treated tumors selectively. 'Back' indicates the fluorescence in the back representing background signal. Data are means ± s.e.m. (n=3). (D) Intratumoral distribution of daunorubicin. Daunorubicin was broadly and homogeneously distributed post-PIT encircling the surviving tumor cells (Balb/DsRed and A431). DsRed: red, DX (daunorubicin): yellow, IR700: green. Scale bars: 100 μm.

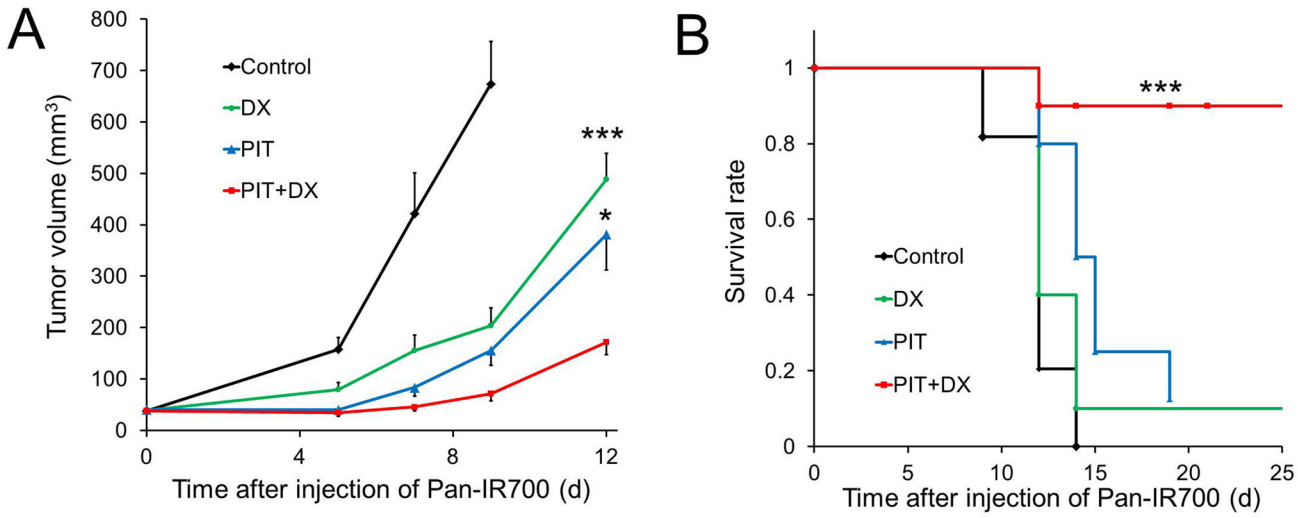

Figure 3.

In vivo therapeutic effect induced by the combination of PIT and liposomal daunorubicin. (A) Tumor growth inhibition by a combination therapy of Pan-IR700-mediated PIT and liposomal daunorubicin in A431 and Balb/DsRed tumors. Data are mean ± s.e.m. n ≥ 10 mice in each group, ***p< 0.01, *p< 0.05 for treatment compared to DX-only groups and PIT-only groups. (B) Analysis using a KaplanMeier survival curve of the combination therapy of PIT and liposomal daunorubicin in A431 and Balb/DsRed tumors. n ≥ 10 mice in each group, ***p< 0.05 for treatment compared to the other control groups using a log-rank test with a Bonferroni's correction for multiple comparisons.